Quantitative proteomic analysis of EZH2 inhibition in acute myeloid leukemia reveals the targets and pathways that precede the induction of cell death

Jarrod J. Sandow[1], Giuseppe Infusini[1], Aliaksei Z. Holik[1], Gabriela Brumatti[1], Tessa V. Averink[1,2,3], Paul G. Ekert[2], Andrew I. Webb[1]

1. The Walter and Eliza Hall Institute of Medical Research, Parkville, VIC 3052, Australia; Department of Medical Biology, The University of Melbourne, Parkville, VIC 3052, Australia.
2. Murdoch Children's Research Institute, Royal Children's Hospital, Parkville, VIC 3052, Australia.
3. Vrije Universiteit, De Boelelaan 1105, 1081HV, Amsterdam

Authors to whom correspondence should be addressed: Dr. Jarrod J. Sandow and Dr. Andrew I. Webb. The Walter and Eliza Hall Institute of Medical Research, 1G Royal Parade, Parkville, VIC 3052, Australia
email: JJS, sandow@wehi.edu.au, Tel: +61-3-93452831; Fax: +61-3-93470852; AIW, webb@wehi.edu.au, Tel: +61-3-93452832; Fax: +61-3-93470852

Abbreviations

PRC2 polycomb repressive complex-2

MLL	mixed-lineage leukemia
EZH2	enhancer of Zeste Homologue 2
AML	acute myeloid leukemia
DZnep	3-Deazaneplanocin A
HSC	hematopoietic stem cells

Keywords
Acute myeloid leukemia, DZnep, EZH2, MLL, PRC2

Word count: 5248 words

ABSTRACT

PURPOSE

Chromosomal translocation of the Mixed Lineage Leukemia (MLL) locus generates fusion proteins that drive acute myeloid leukemia (AML) resulting in atypical histone methyltransferase activity and alterations in the epigenetic regulation of gene expression. Targeting histone regulators, such as Enhancer of Zeste Homologue 2 (EZH2), has shown promise in AML. Profiling differential protein expression following inhibition of epigenetic regulators in AML may help to identify novel targets for therapeutics.

EXPERIMENTAL DESIGN

Murine models of AML combined with quantitative SILAC analysis were used to identify differentially expressed proteins following inhibition of EZH2 activity using 3-Deazaneplanocin A (DZnep). Western blotting and flow cytometry were used to validate a subset of differentially expressed proteins. Gene set analysis was used to determine changes to reported EZH2 target genes.

RESULTS

Our quantitative proteomic analysis and subsequent validation of protein changes identified that epigenetic therapy leads to cell death preceded by the induction of differentiation with concurrent p53 up-regulation and cell cycle arrest. Gene set analysis revealed a specific subset of EZH2 target genes that were regulated by DZnep in AML.

CONCLUSIONS AND CLINICAL RELEVANCE

These discoveries highlight how this new class of drugs affects AML cell biology and cell survival, and may help identify novel targets and strategies to increase treatment efficacy.

STATEMENT OF THE SIGNIFICANCE OF THE STUDY

Current treatments for Acute myeloid leukemia (AML) are limited and ineffective in many patients resulting in poor survival outcomes. Using quantitative proteomics, we characterized global protein expression changes that occur when inhibiting the methyltransferase, EZH2, in AML. We demonstrated that inhibition of EZH2 leads to differentiation of AML cells despite the continued expression of MLL-AF9, the driver oncogene, implicating EZH2 as having a key role in blocking differentiation in these AML sub-types. Inhibition of EZH2 also initiates cell cycle arrest that is characterized by down-regulation of Mki67 protein, regulation of several cyclin-dependent kinase pathways and increased expression of p53, a critical regulator of cell survival and proliferation. Correlation with known EZH2 target genes using Gene Set Enrichment Analysis also identified a distinct set of EZH2 target genes regulated at the protein level when EZH2 is inhibited. This is a key finding as it identifies the unique protein expression changes that occur upon EZH2 inhibition with continued expression of the driver oncogene, a likely scenario when treating patients with inhibitors in the clinic, allowing for the development of clinical biomarkers that can contribute to diagnostic stratification and determination of treatment efficacy.

INTRODUCTION

The polycomb repressive complex-2 (PRC2) regulates the trimethylation of lysine 27 on histone 3 (H3K27me3) to promote transcriptional repression[1]. It is a multi-subunit protein complex that includes SUZ12, EED, RBBP4 and the catalytic subunit Enhancer of Zeste Homologue 2 (EZH2)[2-5]. In the hematopoietic system, high expression of EZH2 conserves the repopulating potential of hematopoietic stem cells[6]. The PRC2 complex has also been shown to contribute to a number of hematopoietic and solid tumors with the outcome of complex deregulation, either tumor promoting or repressing, dependent on the type of disease[7]. Following transformation, ectopic expression of EZH2 in multiple myeloma promotes growth factor independence[8]. In acute myeloid leukemia (AML), PRC2 complex activity has been implicated in supporting disease progression. Studies using murine AML models show that the proliferation and survival of leukaemic cells is dependent on PRC2 complex. Deletion of *Ezh2* inhibited leukemia cell proliferation and knockout of *Eed* completely ablated leukemia self-renewal[9]. This finding was supported by knocking down components of the PRC2 complex in MLL-fusion mouse models of AML leading to longer survival times and differentiation of AML cells in culture[10].

PRC2 is a therapeutic target of considerable importance given the key role this complex plays in driving AML development and maintenance. Experimental and clinical PRC2 inhibitors are being developed and 3-Deazaneplanocin A (DZnep) is a compound that inhibits EZH2 indirectly by competitive inhibition of S-adenosylhomocysteine hydrolase. This leads to an accumulation of adenosylhomocysteine, inhibition of methyltransferases and the subsequent down-regulation of PRC2 levels[11, 12]. Other compounds, such as EI1, EPZ005687 and GSK126, directly target EZH2 by binding to its S-adenosylmethionine pocket leading to growth arrest and apoptosis, even in cells containing activating mutations such as EZH2 Tyr641[13]. DZnep in particular has shown promise as an anti-leukemic agent in pre-clinical models of AML with treatment not only killing leukemic blast cells but also the leukemic stem cell population[14-17].

While it is clear that this complex is required for AML progression there is currently no information on the regulation of cellular protein levels that result from PRC2 complex inhibition. Defining how methyltransferase inhibitors affect cells is important to gather insight into the biological mechanisms of their function, and gain a greater understanding of potential synergies with other drug targets. Such studies may also identify potential drug

resistance mechanisms. We have characterized the response of AML cells to DZnep treatment by measuring and comparing quantitative protein expression profiles. We have identified proteins that may serve as biomarkers of treatment response or that may be targets for novel therapeutics, which function independently or synergistically with DZnep treatment. We have also identified that DZnep treatment leads to the initiation of differentiation and cell cycle arrest in our AML cells before apoptosis is initiated demonstrating a potential mode of action for this class of drugs.

MATERIALS AND METHODS

Generation of mouse AML cells

The TRE-dsRED2-IRES-MLL/AF9 and $NRas^{G12D}$-tTA retroviral vectors have been described previously[18]. A detailed protocol can be found in the supplementary materials and methods. Briefly, fetal liver cells (E14.5) from mice were infected with viral supernatants. After two rounds of infection, cells were injected into sub-lethally irradiated mice. Mice were collected when disease was evident. Leukemic cells were obtained from bone marrow of sick mice. Cells were cultured at 37°C in a 10% CO_2 humidified atmosphere in IMDM media supplemented with 10% fetal calf serum and 5ng/ml Interleukin-3. The *ex vivo* AML cells proliferate rapidly and could be maintained in continuous cell culture. Cells were discarded once they had reached 20 passages to prevent the accumulation of mutations in culture.

SILAC labeling of AML cells and treatment with DZnep

Isolated *ex vivo* AML cells from 3 independently generated leukemias (independent retroviral transduction and independent recipient mice) were cultured in lysine and arginine free IMDM supplemented with either normal or heavy (L-Lysine-$^{13}C_6$,$^{15}N_2$ hydrochloride, L-Arginine-$^{13}C_6$, $^{15}N_4$ hydrochloride) lysine and arginine (Sigma-Aldrich, USA) for at least 5 passages prior to the experiment to achieve >98% incorporation of isotopic amino acids with the percentage of heavy amino acid incorporation determined by analysis of heavy labeled samples alone prior to mixing. Cells were then either treated with 1µM DZnep (Cayman Chemicals, USA) or vehicle (DMSO) for 16 hours. Proteins were collected by boiling cell pellets in 4% SDS, 100mM Tris-HCl pH7.4, 100mM DTT for 10min.

Peptide sample preparation

Samples (100µg) were resuspended in 6M Urea, 100 mM DTT and 100 mM Tris-HCl pH7.0 and subjected to protein digestion using a FASP (filter aided sample preparation) column[19] (Expedeon Inc., CA, USA). Solvent was removed by lyophilization before resuspension of peptides in Britton & Robinson Universal Buffer (20mM CH_3COOH, 20mM H_3PO_4, 20mM H_3BO_4) pH12. Peptides were separated into 6 fractions using strong anion exchange (SAX) as described previously [19] using pH12, 8, 6, 5, 4, 2 in a SAX/C_{18} StageTip format.

Mass Spectrometry analysis

Peptides were resuspended in 3% acetonitrile (ACN) and 0.1% formic acid (FA) (100ng/ul). Samples were analyzed by nanoflow LC-MS/MS on a nanoAcquity system (Waters, Milford, MA, USA) coupled to a Q-Exactive mass spectrometer (Thermo Fisher Scientific, Bremen, Germany) through a nanoelectrospray ion source (Thermo Fisher Scientific). Peptide mixtures were loaded on a 20mm trap column with 180µm inner diameter (nanoAcquity UPLC 2G-V/MTrap 5µm Symmetry C18) at 1% buffer B, and separated by reverse-phase chromatography using a 150mm column with 75µm inner diameter (nanoAcquity UPLC 1.7µm BEH130 C18) on a 120 minute linear gradient from 1% to 35% buffer B (A: Milli-Q water, 3% ACN, 0.1% FA; B: 99.9% ACN, 0.1% FA) at a 500nl/min constant flow rate. The Q-Exactive was operated in a data-dependent mode, switching automatically between one full-scan and subsequent MS/MS scans of the ten most abundant peaks. The instrument was controlled using Exactive series version 2.1 build 1502 and Xcalibur 3.0. Full-scans (m/z 350–1,850) were acquired with a resolution of 70,000 at 200 m/z. The 10 most intense ions were sequentially isolated with a target value of 10000 ions and an isolation width of 3 m/z and fragmented using HCD with NCE of 27. Maximum ion accumulation times were set to 50ms for full MS scan and 150ms for MS/MS.

Statistical analysis

Raw files were analysed using MaxQuant[20, 21] (version 1.4.1.2), The database search was performed using the Ludwig NR protein database (version Q114, http://www.wehi.edu.au/faculty/advanced_research_technologies/proteomics/wehi_systems_biology_mascot_server/) with strict trypsin specificity allowing up to 2 missed cleavages. The minimum peptide length was 7 amino acids. Carbamidomethylation of cysteine was a fixed modification while N-acetylation of proteins N-termini, oxidation of

methionine and pyroglutamate at peptides N-termini Glu and Gln were set as variable modifications. During the MaxQuant main search, precursor ion mass error tolerance was set to 4.5 ppm and fragment ions were allowed a mass deviation of 20 ppm. PSM and protein identifications were filtered using a target-decoy approach at a false discovery rate (FDR) of 1% with the match between runs option was enabled. Further analysis was performed using a custom pipeline developed in Pipeline Pilot (Biovia) with details provided in supplementary materials and methods.

Analysis of cell viability and validation of protein expression

Cell viability was determined as described previously[22]. A detailed protocol of flow cytometry and Western blotting protocols and reagents can be found in supplementary materials and methods. Briefly, cells were stained with propidium iodide followed by flow cytometric analysis with viable cells identified by their ability to exclude PI. Expression of surface and intra-cellular antigens was determined using fluorochrome conjugated antibodies followed by flow cytometry.

RESULTS AND DISCUSSION

DZnep treatment of AML cells results in cell death

DZnep has shown promise as a therapeutic compound in several different models of cancer[12, 14, 23]. AMLs harboring rearrangements at 11q23 are known to be sensitive to disruption and inhibition of the PRC2 complex[9]. Given the clinical significance of PRC2 inhibition we sought to profile the changes in protein expression following inhibition of the PRC2 complex using DZnep, an inhibitor of methyltransferases including the PRC2 catalytic component, EZH2. To generate AML cells *in vivo* we used retroviral constructs that result in the over-expression of MLL-AF9 and a constitutively active $NRas^{G12D}$ mutant with dsRED also expressed as a fluorescent marker (Figure 1A). AML was induced in mice by transducing E14.5 fetal liver hematopoietic stem cells (HSC) with the retroviral constructs before reconstitution of lethally irradiated recipient mice with the transduced cells. Mice succumbed to AML with a median time to death of 18 days post-reconstitution (Figure 1B) commonly presenting with weight-loss, splenomegaly, anemia, lethargy and hunched posture. Control mice transduced with GFP alone did not develop AML within the time period of the experiment. Blood profile analysis at the time of death revealed that mice reconstituted with MLL-AF9;$NRas^{G12D}$ had elevated white blood cells counts (Figure 1C) and

reduced platelet counts (Figure 1D) compared to control mice. AML cells were harvested from the bone marrows of leukemic mice and grown in liquid culture *ex vivo*. To determine the ability of DZnep to kill the AML cells *ex vivo* by inhibiting EZH2 and disrupting the PRC2 complex we treated cells with DZnep at a range of concentrations or with DMSO as a vehicle control before measurement of cell viability using propidium iodide exclusion (Figure 1E). Following 24 hours of DZnep treatment, cell viability fell to around 30% when exposed to 100nM DZnep and around 10% viability after 1000nM DZnep. These results characterise the MLL-AF9;NRas^{G12D} AML models and show that inhibition of EZH2 using DZnep effectively kills AML cells transformed with MLL-AF9.

Quantitative analysis of protein expression following treatment of AML cells with DZnep

The PRC2 complex acts on gene expression by regulating transcription (and indirectly translation) of target genes. Therefore, we sought to profile the changes in protein expression following disruption of PRC2 activity using the EZH2 inhibitor, DZnep. To achieve this, MLL-AF9 transformed AML cells were isolated and cultured *ex vivo* as described above. Cells were labelled in 'light' or 'heavy' SILAC medium supplemented with IL-3 (see materials and methods). Cells were then treated for 16 hours with either 1µM DZnep or DMSO as a vehicle control before lysis, tryptic digest and mass spectrometric analysis. A schematic of the experimental workflow is shown in Figure 2A. The database search identified 32,053 peptides and 5,410 proteins with a peptide spectrum match false discovery rate set at 1% (see 'materials and methods'). Of the proteins identified, 4,321 had at least two or more razor + unique peptides. Statistical analysis of changes in protein expression across the three independent biological replicates based on peptide SILAC ratios demonstrated that 2,922 proteins had a p-value ≤0.05. The distribution of fold-change *versus* p-values is demonstrated as a volcano plot in Figure 2B. Of proteins with a p-value ≤0.05 and a fold-change ≥1.5 where more than one unique peptide was identified, 68 proteins were up-regulated and 76 proteins were down-regulated (Supplementary table 1). These results demonstrate that there are significant changes in protein expression within 16 hours of exposure to DZnep as AML cells begin to respond to treatment and undergo apoptosis.

Functional analysis of changes in protein expression

We submitted the differentially expressed gene lists for Gene Ontology analysis using the PANTHER classification system[24] (Figure 3A and 3B). Although it is likely that cells had initiated early commitment to apoptotic processes when protein was collected we did not observe significant changes in proteins involved in cell death or survival in our analysis. This

probably reflects the fact that altered activation or repression of apoptosis is not necessarily indicated by changes in protein expression levels but by activation or repression of functional status such as protein post-translational modification or cleavage of proteins into pro-apoptotic fragments. One class of proteins that was significantly down-regulated was proteins involved in nucleic acid binding (Figure 3A). This is consistent with the activity of DZnep as an EZH2 inhibitor and other methyltransferases that are responsible for epigenetic modification of DNA that contribute to protein interactions with DNA[11]. One of these nuclear binding proteins, TOP2A, is significantly down-regulated (1.6-fold) in our proteomic data following DZnep treatment (Supplementary Figure 1). However, when we attempted to validate our observation using Western blotting we were unable to detect TOP2A in either the untreated AML cells or cells treated with DZnep, which is likely due to a limitation with current TOP2A antibodies (Figure 4A). We were only able to observe TOP2A by Western blot when the cells were treated using the DNA damaging chemotherapeutic compound, etoposide (Figure 4A). High expression of TOP2A has been demonstrated in aggressive prostate cancer and non-small-cell lung cancer as a marker of poor survival outcome and it is known to functionally interact with EZH2 to promote oncogenesis. Co-inhibition of each enzyme using the combined treatment of etoposide (TOP2A) and DZnep (EZH2) in these cancers leads to a synergistic increase in cell death, significantly improved reduction in tumor burden and increased overall survival outcomes in preclinical models[25, 26]. Given that DZnep treatment in our MLL-AF9 leukemic model leads to reduced levels of the main target for etoposide, TOP2A, it will be important to investigate if reduced TOP2A protein levels promote or reduce the effectiveness of the drug combination if a similar strategy were considered in AML.

There were a number of protein classes that were either enriched or only present in the up-regulated proteins including cell adhesion molecules, enzyme modulators, defense/immunity proteins and receptors (Figure 3A). Analysis of biological processes associated with up-regulated expression of genes included immune system process, response to stimulus, developmental process and biological adhesion (Figure 3B). The pattern of protein classes and biological processes is commonly associated with HSC differentiation such as FCGR2 (CD32; 2.31-fold) and ITGAM (CD11b; 1.75-fold), all markers of mature myeloid lineages (Supplementary Figure 1). We confirmed this observation by measuring the cell surface expression of these proteins in addition to another mature myeloid cell marker, Gr-1, following DZnep treatment using flow cytometry. We observed an increase in the cell surface expression of ITGAM, CD16/32 and Gr-1 following DZnep treatment (Figure 4B). Together, this data suggests that disruption of PRC2 in the context of the MLL-AF9 leukemic model results in the release of a blocked differentiation program.

This discovery complements published results that demonstrate deletion of EZH2 in AML driven by MLL-AF9 leads to less blast cells in the bone marrow and periphery, an increase in differentiated colonies as well as a lower frequency of leukemia initiating cells[17]. In addition to increases in differentiation markers following DZnep treatment we also observed a significant fall in Mki67 expression (2-fold), a key marker of cell proliferation [27] (Supplementary Figure 1). We validated this data by using flow cytometry to observe that levels of Mki67 fell by half following treatment with DZnep (Figure 4C). While these results demonstrate that AML cells treated with DZnep undergo differentiation and cell cycle arrest before the induction of apoptosis, we also identify cell surface proteins that are up-regulated following drug treatment, which may provide novel clinical biomarkers for treatment efficacy where PRC2 complex inhibition is being employed.

DZnep regulates expression of proteins that are known to contribute to leukemogenesis.

We also analyzed the changes in expression of proteins that are known to contribute to AML. The cyclin-dependent kinases, CDK1 and CDK6, regulate cell cycle and viability and our results demonstrate that they were down-regulated upon DZnep treatment (1.63 and 1.85-fold respectively; Supplementary Figure 1). We validated the decrease of both CDK1 and CDK6 protein levels following the treatment DZnep using Western blotting (Figure 4A). CDK6 is known to be up-regulated by MLL fusion proteins in acute lymphoblastic leukemia where it acts as a critical contributor to the proliferative advantage of cells expressing these oncogenes[28]. The regulation of CDK6 expression by EZH2 has been observed in glioblastoma cells where microRNAs or specific siRNA constructs targeting EZH2 lead to loss of CDK6 protein expression[29]. The down-regulation of CDK6 expression following DZnep treatment suggests that EZH2 may also regulate CDK6 in our AMLs models, even when MLL fusion protein expression is present. While the regulation of CDK1 protein expression by EZH2 is not well understood, CDK1 is known to directly phosphorylate EZH2, leading to ubiquitination and degradation of EZH2[30, 31]. An additional mechanism used by cells to regulate CDK activity is direct inhibition by CDKN1A (also known as p21), a protein that is expressed in response to p53 activation[32]. Our proteomic results demonstrate that CDKN1A is up-regulated (1.52-fold) in response to DZnep treatment which would lead to inhibition of CDK1, CDK4 and CDK6 activity and inhibition of cell cycle progression (Supplementary figure 1). As *Cdkn1a* is a p53 response gene this result also indicates that activation of p53 may play an important role in AML cells response to treatment with DZnep. To support this hypothesis, we used Western blotting to determine the change in protein levels of CDKN1A and p53 following DZnep treatment. Following DZnep treatment we were able to observe an up-regulation of both CDKN1A and p53 (Figure 4A). As a positive control for a p53 activity we treated our AML cells with etoposide, a drug known to activate

the p53-dependent cell death pathway[33]. This also resulted in an up-regulation of CDKN1A and p53 (Figure 4A). The role of p53 and CDKN1A in the response to DZnep is therapeutically important as only a minority (around 6%) of AMLs that are driven by MLL-translocations contain additional p53 inactivating mutations[34]. This suggests that p53-dependent apoptosis can be activated in the treatment of these AMLs. Other kinases such as Aurora Kinase A and Aurora Kinase B were also down-regulated in our proteomic results upon treatment with DZnep (1.75 and 1.72- fold respectively; Supplementary figure 1). Western blotting confirmed that Aurora Kinase A was down-regulated by DZnep treatment (Figure 4A). This result complements published observations in breast cancer which showed that over-expression of EZH2 lead to increased protein levels of Aurora Kinase A and Aurora Kinase B, while knockdown of EZH2 resulted in loss of expression of these proteins resulting in abnormal mitosis[35]. Taken together these results demonstrate that treatment of AML cells with DZnep regulates the expression of a diverse range of proteins that are known EZH2 targets and have been previously implicated in a broad range of cancers, including leukemia.

Changes in protein abundance overlap with a subset of EZH2 target genes

We anticipated that the direct targets of the PRC2 complex would selectively increase in expression in response to DZnep treatment as a consequence of the reduced trimethylation of H3K27, an inhibitory mark for gene expression. To determine if expression changes induced by EZH2 inhibition were associated with EZH2 binding, we obtained a list of 4007 genes from 15 different cell lines from the ENCODE project found to harbor EZH2 binding sites in their promoter region. Highlighting the EZH2 target genes indicates that there were a substantial number of EZH2 target genes that were up-regulated following DZnep treatment, as would be anticipated (Figure 5A). Gene set analysis of this list revealed that EZH2 target genes were significantly over-represented among the genes that increased their expression in response to EZH2 inhibition (p-value<0.0005; Figure 5B). This observation supports the role of PRC2 as a repressive complex with inhibition of the complex resulting in the up-regulation of direct targets. Many other known EZH2 targets did not change their expression and there were also a number of genes that appear down-regulated upon DZnep treatment which may represent an indirect effect of EZH2 inhibition[36]. The MLL-AF9 fusion protein is known to interact with a number of methyltransferases to regulate gene expression[37]. Therefore, the observed changes in protein expression are a unique result of the combination of methyltransferases associated with MLL-AF9 and DZnep treatment and not simply canonical EZH2 targets. The changes in expression of the top 20 EZH2 target genes (identified with >1 unique peptide) are summarized in Table 1 with the complete list published in supplementary table 2.

Analysis of proteins involved in the PRC2 complex including SUZ12, EED and RBBP4 (EZH2 was not reproducibly identified) indicated that their expression did not undergo significant change over the course of the experiment (Supplementary Figure 1). An inhibitory regulator of PRC2 activity, JARID2, was up-regulated (1.51-fold; Supplementary Figure 1) in response to DZnep treatment. Increased expression of JARID2 is likely to further reduce the effect of PRC2 on target gene repression. Analysis of EZH2 and SUZ12 protein expression using Western blotting confirmed that their levels did not change following DZnep treatment while levels of JARID2 were increased (Figure 4A). These results suggest that it is an inhibition of EZH2 activity rather that a loss of EZH2 protein expression that appears to be driving the changes to the AML proteome following DZnep treatment.

Concluding remarks

AML is a devastating disease with limited treatment options. We have demonstrated using SILAC quantitative mass spectrometry that targeting EZH2 in AML using a pre-clinical compound, DZnep, results in cell death that is preceded by cell cycle arrest, a release from oncogene induced differentiation blockage and up-regulation of mature cell lineage markers. This is a key finding as it demonstrates that EZH2 plays an important role in blocking differentiation in leukemia, as MLL-AF9 expression is still present during DZnep treatment. Characterizing the response of target cells to treatment with therapeutics is an important step in understanding how these compounds induce death in specific cells and may provide clinical biomarkers for treatment efficacy. Given the differing role of EZH2 in cancer, either tumor-suppressing or promoting, this analysis also provides insight into the disease specific role of this complex and identifies the regulation of key proteins that allow EZH2 to promote leukemogenesis.

ACKNOWLEDGMENTS

This work was supported by NHMRC project grants #1025594, #1081376. GB is supported by Victorian Cancer Agency, Mid-career fellowship. This work was made possible through Victorian State Government Operational Infrastructure Support, and L.E.W. Carty Charitable Fund and Ian Rollo Currie Estate Foundation for infrastructure support.

CONFLICT OF INTEREST STATEMENT

The authors declare no competing financial interests.

REFERENCES

[1] Kirmizis, A., Bartley, S. M., Kuzmichev, A., Margueron, R.*, et al.*, Silencing of human polycomb target genes is associated with methylation of histone H3 Lys 27. *Genes & development* 2004, *18*, 1592-1605.

[2] Cao, R., Wang, L., Wang, H., Xia, L.*, et al.*, Role of histone H3 lysine 27 methylation in Polycomb-group silencing. *Science (New York, N.Y.)* 2002, *298*, 1039-1043.

[3] Czermin, B., Melfi, R., McCabe, D., Seitz, V.*, et al.*, Drosophila enhancer of Zeste/ESC complexes have a histone H3 methyltransferase activity that marks chromosomal Polycomb sites. *Cell* 2002, *111*, 185-196.

[4] Kuzmichev, A., Nishioka, K., Erdjument-Bromage, H., Tempst, P., Reinberg, D., Histone methyltransferase activity associated with a human multiprotein complex containing the Enhancer of Zeste protein. *Genes & development* 2002, *16*, 2893-2905.

[5] Kuzmichev, A., Jenuwein, T., Tempst, P., Reinberg, D., Different EZH2-containing complexes target methylation of histone H1 or nucleosomal histone H3. *Molecular cell* 2004, *14*, 183-193.

[6] Kamminga, L. M., Bystrykh, L. V., de Boer, A., Houwer, S.*, et al.*, The Polycomb group gene Ezh2 prevents hematopoietic stem cell exhaustion. *Blood* 2006, *107*, 2170-2179.

[7] Chase, A., Cross, N. C., Aberrations of EZH2 in cancer. *Clinical cancer research : an official journal of the American Association for Cancer Research* 2011, *17*, 2613-2618.

[8] Croonquist, P. A., Van Ness, B., The polycomb group protein enhancer of zeste homolog 2 (EZH 2) is an oncogene that influences myeloma cell growth and the mutant ras phenotype. *Oncogene* 2005, *24*, 6269-6280.

[9] Neff, T., Sinha, A. U., Kluk, M. J., Zhu, N.*, et al.*, Polycomb repressive complex 2 is required for MLL-AF9 leukemia. *Proceedings of the National Academy of Sciences of the United States of America* 2012, *109*, 5028-5033.

[10] Shi, J., Wang, E., Zuber, J., Rappaport, A.*, et al.*, The Polycomb complex PRC2 supports aberrant self-renewal in a mouse model of MLL-AF9;Nras(G12D) acute myeloid leukemia. *Oncogene* 2013, *32*, 930-938.

[11] Miranda, T. B., Cortez, C. C., Yoo, C. B., Liang, G.*, et al.*, DZNep is a global histone methylation inhibitor that reactivates developmental genes not silenced by DNA methylation. *Molecular cancer therapeutics* 2009, *8*, 1579-1588.

[12] Tan, J., Yang, X., Zhuang, L., Jiang, X*., et al.*, Pharmacologic disruption of Polycomb-repressive complex 2-mediated gene repression selectively induces apoptosis in cancer cells. *Genes & development* 2007, *21*, 1050-1063.

[13] Qi, W., Chan, H., Teng, L., Li, L*., et al.*, Selective inhibition of Ezh2 by a small molecule inhibitor blocks tumor cells proliferation. *Proceedings of the National Academy of Sciences of the United States of America* 2012, *109*, 21360-21365.

[14] Ueda, K., Yoshimi, A., Kagoya, Y., Nishikawa, S*., et al.*, Inhibition of histone methyltransferase EZH2 depletes leukemia stem cell of MLL fusion leukemia through up-regulation of p16. *Cancer science* 2014.

[15] Fiskus, W., Wang, Y., Sreekumar, A., Buckley, K. M*., et al.*, Combined epigenetic therapy with the histone methyltransferase EZH2 inhibitor 3-deazaneplanocin A and the histone deacetylase inhibitor panobinostat against human AML cells. *Blood* 2009, *114*, 2733-2743.

[16] Zhou, J., Bi, C., Cheong, L. L., Mahara, S*., et al.*, The histone methyltransferase inhibitor, DZNep, up-regulates TXNIP, increases ROS production, and targets leukemia cells in AML. *Blood* 2011, *118*, 2830-2839.

[17] Tanaka, S., Miyagi, S., Sashida, G., Chiba, T*., et al.*, Ezh2 augments leukemogenicity by reinforcing differentiation blockage in acute myeloid leukemia. *Blood* 2012, *120*, 1107-1117.

[18] Zuber, J., Radtke, I., Pardee, T. S., Zhao, Z*., et al.*, Mouse models of human AML accurately predict chemotherapy response. *Genes & development* 2009, *23*, 877-889.

[19] Wisniewski, J. R., Zougman, A., Mann, M., Combination of FASP and StageTip-based fractionation allows in-depth analysis of the hippocampal membrane proteome. *Journal of proteome research* 2009, *8*, 5674-5678.

[20] Cox, J., Mann, M., MaxQuant enables high peptide identification rates, individualized p.p.b.-range mass accuracies and proteome-wide protein quantification. *Nature biotechnology* 2008, *26*, 1367-1372.

[21] Cox, J., Neuhauser, N., Michalski, A., Scheltema, R. A*., et al.*, Andromeda: a peptide search engine integrated into the MaxQuant environment. *Journal of proteome research* 2011, *10*, 1794-1805.

[22] Sandow, J. J., Jabbour, A. M., Condina, M. R., Daunt, C. P*., et al.*, Cytokine receptor signaling activates an IKK-dependent phosphorylation of PUMA to prevent cell death. *Cell death and differentiation* 2012, *19*, 633-641.

[23] Gaudichon, J., Milano, F., Cahu, J., DaCosta, L.*, et al.*, Deazaneplanocin a is a promising drug to kill multiple myeloma cells in their niche. *PloS one* 2014, *9*, e107009.

[24] Mi, H., Muruganujan, A., Thomas, P. D., PANTHER in 2013: modeling the evolution of gene function, and other gene attributes, in the context of phylogenetic trees. *Nucleic acids research* 2013, *41*, D377-386.

[25] Kirk, J. S., Schaarschuch, K., Dalimov, Z., Lasorsa, E.*, et al.*, Top2a identifies and provides epigenetic rationale for novel combination therapeutic strategies for aggressive prostate cancer. *Oncotarget* 2015, *6*, 3136-3146.

[26] Fillmore, C. M., Xu, C., Desai, P. T., Berry, J. M.*, et al.*, EZH2 inhibition sensitizes BRG1 and EGFR mutant lung tumours to TopoII inhibitors. *Nature* 2015, *520*, 239-242.

[27] Scholzen, T., Gerdes, J., The Ki-67 protein: from the known and the unknown. *Journal of cellular physiology* 2000, *182*, 311-322.

[28] van der Linden, M. H., Willekes, M., van Roon, E., Seslija, L.*, et al.*, MLL fusion-driven activation of CDK6 potentiates proliferation in MLL-rearranged infant ALL. *Cell cycle (Georgetown, Tex.)* 2014, *13*, 834-844.

[29] Qiu, S., Huang, D., Yin, D., Li, F.*, et al.*, Suppression of tumorigenicity by microRNA-138 through inhibition of EZH2-CDK4/6-pRb-E2F1 signal loop in glioblastoma multiforme. *Biochimica et biophysica acta* 2013, *1832*, 1697-1707.

[30] Wu, S. C., Zhang, Y., Cyclin-dependent kinase 1 (CDK1)-mediated phosphorylation of enhancer of zeste 2 (Ezh2) regulates its stability. *The Journal of biological chemistry* 2011, *286*, 28511-28519.

[31] Zeng, X., Chen, S., Huang, H., Phosphorylation of EZH2 by CDK1 and CDK2: a possible regulatory mechanism of transmission of the H3K27me3 epigenetic mark through cell divisions. *Cell cycle (Georgetown, Tex.)* 2011, *10*, 579-583.

[32] Li, Y., Jenkins, C. W., Nichols, M. A., Xiong, Y., Cell cycle expression and p53 regulation of the cyclin-dependent kinase inhibitor p21. *Oncogene* 1994, *9*, 2261-2268.

[33] Fritsche, M., Haessler, C., Brandner, G., Induction of nuclear accumulation of the tumor-suppressor protein p53 by DNA-damaging agents. *Oncogene* 1993, *8*, 307-318.

[34] Grossmann, V., Schnittger, S., Poetzinger, F., Kohlmann, A.*, et al.*, High incidence of RAS signalling pathway mutations in MLL-rearranged acute myeloid leukemia. *Leukemia* 2013, *27*, 1933-1936.

[35] Gonzalez, M. E., DuPrie, M. L., Krueger, H., Merajver, S. D.*, et al.*, Histone methyltransferase EZH2 induces Akt-dependent genomic instability and BRCA1 inhibition in breast cancer. *Cancer research* 2011, *71*, 2360-2370.

[36] Ferrari, K. J., Scelfo, A., Jammula, S., Cuomo, A.*, et al.*, Polycomb-dependent H3K27me1 and H3K27me2 regulate active transcription and enhancer fidelity. *Molecular cell* 2014, *53*, 49-62.

[37] Li, B. E., Ernst, P., Two decades of leukemia oncoprotein epistasis: the MLL1 paradigm for epigenetic deregulation in leukemia. *Experimental hematology* 2014, *42*, 995-1012.

FIGURE LEGENDS

Figure 1. Expression of MLL-AF9 initiates a leukemia that undergoes apoptosis following treatment with DZnep. (A) Schematic of the retroviral constructs that were used to generate AML in mice. (B) Kaplan-Meier survival curves of mice reconstituted with either MLL-AF9;NRas^{G12D} (n=6) or GFP (n=4) transduced HSC. (C and D) Analysis of total white blood cell (WBC) counts and circulating platelet (PLT) levels in the peripheral blood ±SEM at time of death (MLL-AF9;NRas^{G12D} mice) or at the conclusion of the experiment (GFP mice, 100 days). (E) MLL-AF9;NRas^{G12D} AML cells cultured *ex vivo* were treated with increasing concentrations of DZnep (n=4). Cell viability was analyzed by measuring PI exclusion after 24 hours of treatment. Error bars are + SEM.

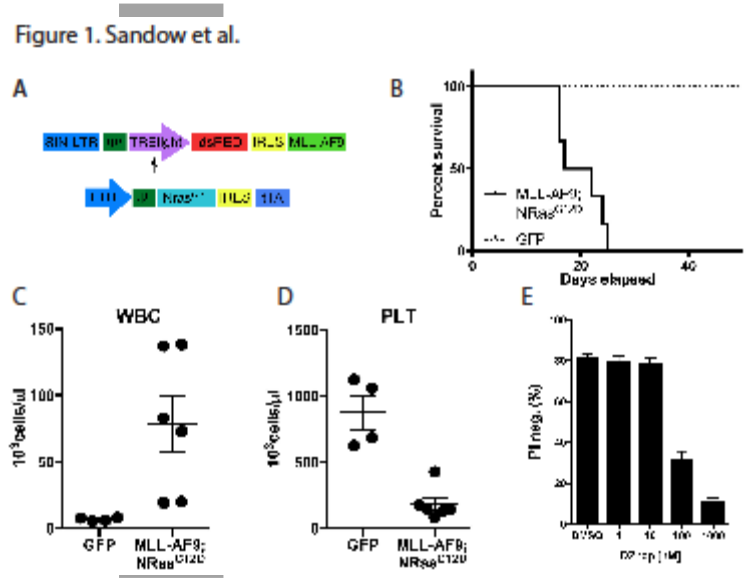

Figure 2. Proteome analysis of AML cells treated with DZnep. (A) Schematic of experiment. Lethally irradiated recipient mice were reconstituted with HSC transduced with MLL-AF9;NRas^{G12D}. Once mice had succumbed to disease, AML cells were harvested form the bone marrow and grown *ex vivo* in tissue culture. Cells were equally divided and grown in either 'light' or 'heavy' SILAC culture medium. Cells were treated with either DZnep or vehicle before being combined in a 1:1 ratio and lysed. Cellular proteins underwent tryptic digestion before SAX fractionation and LC-MS/MS analysis. Raw data was searched using MaxQuant and statistical analysis performed using a custom analysis pipeline. (B) Quantitative analysis of AML cells treated with DZnep or vehicle. Volcano plot representation of relative protein abundance changes upon DZnep treatment. Vertical lines represent 1.5 fold change, horizontal line represents a p-value of 0.05.

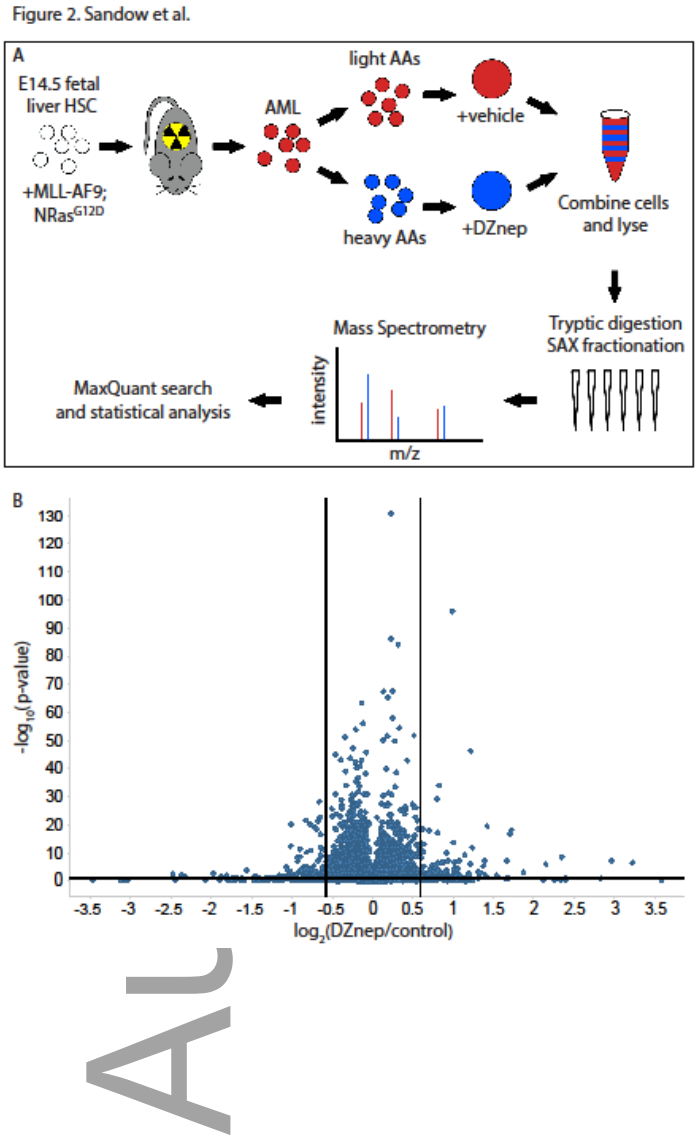

Figure 3. Gene Ontology analysis of the global proteome from DZnep treated AML cells reveals changes to a number of different (A) Protein Classes and (B) Biological processes.

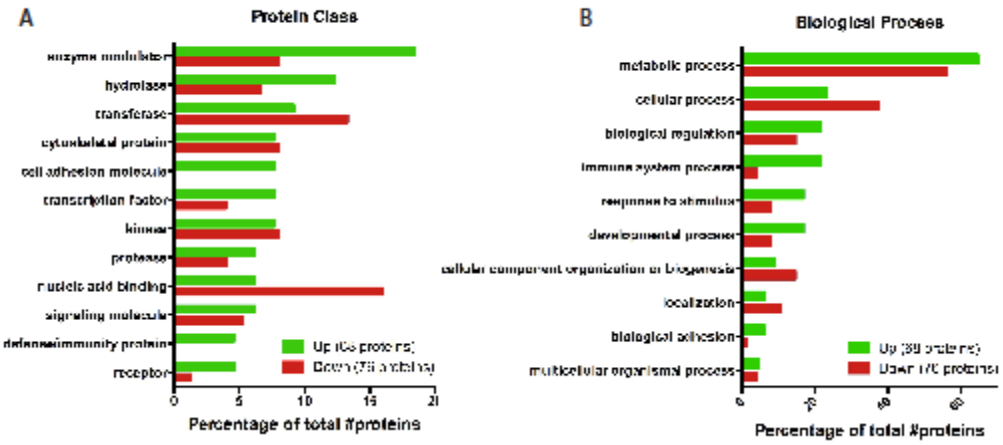

Figure 4. Validation of changes in protein expression from proteomic data. (A) AML cells were treated with either DZnep (100nM or 500nM), vehicle (Vh) or etoposide (Et) for 16 hours. Cells were lysed and analyzed by Western blotting using antibodies against CDK1, CDK6, AURKA, TOP2A, CDKN1A, p53, EZH2, SUZ12, JARID2 and β-actin. (B) AML cells were treated with DZnep (either vehicle, 100nM or 500nM) for 16 hours. The cell surface marker proteins ITGAM, CD16/32 and Gr-1 were quantified using flow cytometry. (C) AML cells were treated with DZnep as described in (B). Cells were fixed and permeabilized before intra-cellular levels of Mki67 were quantified using flow cytometry.

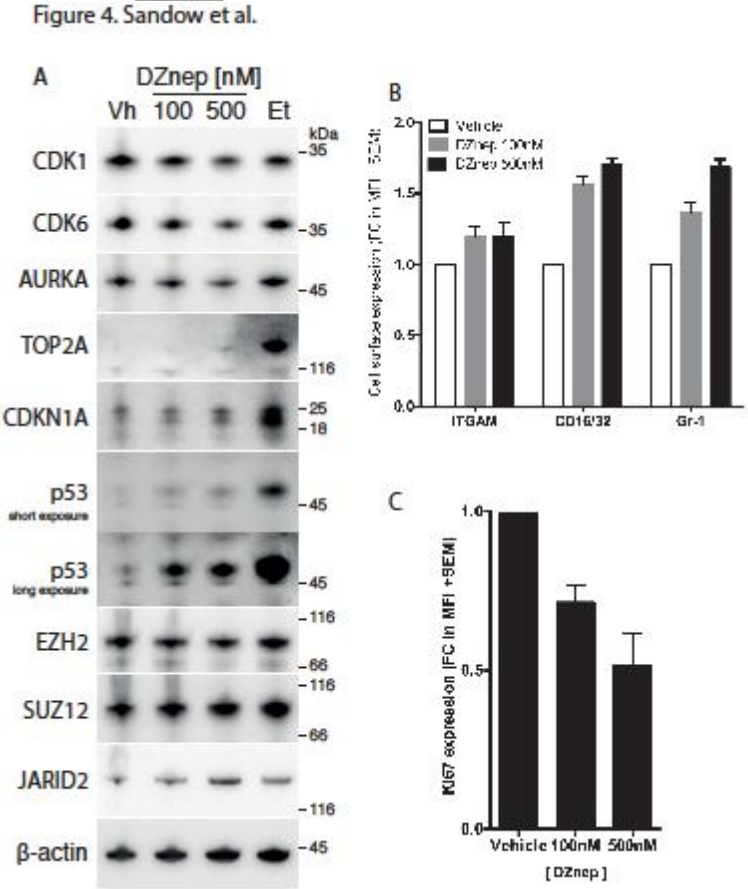

Figure 5. Distribution of EZH2 target genes in relation to expression changes upon EZH2 inhibition. (A) Volcano plot representation of relative protein abundance changes upon DZnep treatment with proteins corresponding to identified EZH2 target genes highlighted. Vertical lines represent 1.5 fold change, horizontal line represents a p-value of 0.05. (B) Gene Set Enrichment Analysis of protein expression from AML cells reveals that EZH2 target gene expression was predominantly up-regulated in DZnep treated cells. Genes are ranked by the log10-transformed expression p-value, signed according to the direction of the expression change. Vertical bars mark EZH2 target genes. Red and blue areas contain the up- or down-regulated genes respectively with a p-value<0.05. The curve above the plot represents moving density of the Ezh2 target genes across the range of expression changes.

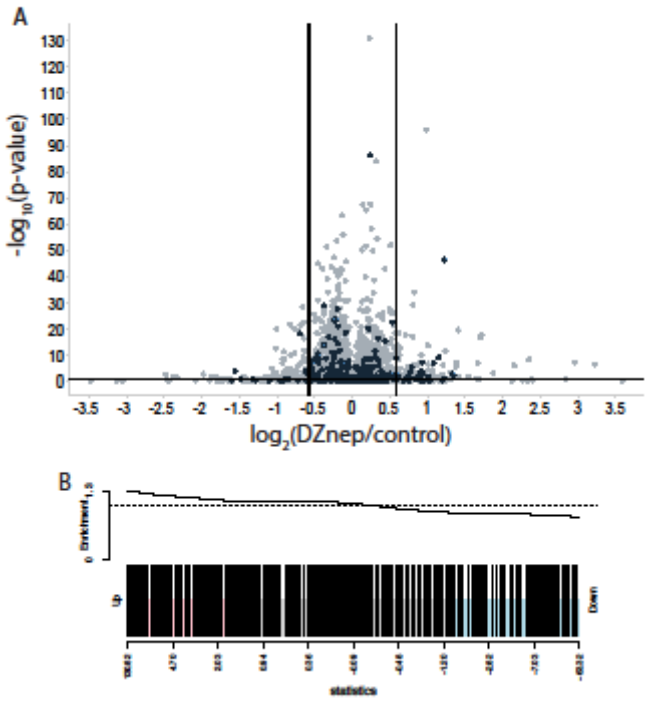

Table 1. Changes in abundance of the top 20 up-regulated proteins that correspond to EZH2 target genes.

Accession number	Gene Names	Protein Names	Protein Ratio H/L Normalized	P-Value Normalized	Unique Peptides	Unique sequence coverage (%)	Coefficient of Variation (%)
Q00322	Cebpd	CCAAT/enhancer-binding protein delta	2.538	0.0011655011655	2	19	23.58
P17156	Hspa2	Heat shock-related 70 kDa protein 2	2.325	4.1097037563E-47	17	38.1	13.55
Q6ZWR6-4	Syne1	Nesprin-1	2.2089	4.2589346448E-10	15	4.5	43.47
ENSMUSP00000115456	Ak4	GTP:AMP phosphotransferase AK4	2.116	4.9854673626E-08	4	42.6	8.69
Q8C9E4	Ly9	T-lymphocyte surface antigen Ly-9	2.0217	0.0079365079365	2	10.8	11.68
Q922Q7	Ctsh	Cathepsin H	1.9106	4.9854673626E-08	3	19.8	28.46
ENSMUSP00000130883	Ncam1	Neural cell adhesion molecule 1	1.89955	0.0021645021645	3	9.4	15.40
ENSMUSP00000098893	Nhsl2	NHS-like protein 2	1.8924	8.2270670506E-05	3	8.2	30.09
ENSMUSP00000128746	Abhd14b	Alpha/beta hydrolase domain-containing protein 14B	1.7271	2.835142154E-06	3	27.3	28.50
Q3TJD7	Pdlim7	PDZ and LIM domain protein 7	1.6649	0.0079365079365	2	7.4	4.43
Q564P6	Cdkn1a	Cyclin-dependent kinase inhibitor 1	1.5182	0.0079365079365	2	30.8	12.44
G3UZT8	Jarid2	Protein Jumonji	1.51305	0.028571428571	2	3.5	26.42
Q9D1Q3	Itm2b	Integral membrane	1.5006	8.5704262478E-	4	33.5	

		protein 2B		10			21.51
Q64314-2	Cd34	Hematopoietic progenitor cell antigen CD34	1.4878	0.0012340600576	2	10.2	9.47
Q9CQI6	Cotl1	Coactosin-like protein	1.44115	1.8603403656E-23	6	55.6	15.17
P47930-2	Fosl2	Fos-related antigen 2	1.421	0.0079365079365	2	5.7	3.56
Q9Z2Q6	Sept5	Septin-5	1.40835	0.0015046872632	2	12.2	13.8
Q9QZ82	Cyp11a1	Cholesterol side-chain cleavage enzyme	1.4057	0.038721138869	5	16	44.10
Q6ZWX2	Tmsb4x	Thymosin beta-4	1.3517	1.3822839071E-16	3	75	3.69
F7C957	Pdlim2	PDZ and LIM domain protein 2	1.3451	0.0010878011	2	22.5	1.21